Laser and Particle Beams (2016), *34*, 72–79.

doi:10.1017/S0263034615000920

Self-pumped SBS effect of high-power super-Gaussian-shaped laser pulses

YULEI WANG,[†] XUEHUA ZHU,[†] ZHIWEI LU, AND HENGKANG ZHANG

National Key Laboratory of Science and Technology on Tunable Laser, Harbin Institute of Technology, Harbin 150080, China

(RECEIVED 19 April 2015; ACCEPTED 13 October 2015)

Abstract

Most of the high-energy laser systems deliver temporally super-Gaussian-shaped laser pulses. The propagation properties of this kind of pulses in a nonlinear medium are studied in this paper. There is Stokes component in the sideband spectrum of super-Gaussian-shaped pulses, and the frequency difference between the Stokes component and the center frequency is equals to the Brillouin frequency of the nonlinear medium. When the laser is reflected by optical elements in the light path, Stokes component in the reflected light can be amplified by the subsequent part of the laser pulse and excite stimulated Brillouin scattering (self-pumped SBS). The self-pumped SBS is studied theoretically and experimentally, and the experimental results agreed well with the calculated results. The simulation results show that lower-order super-Gaussian-shaped pulses are more suitable for suppressing the self-pumped SBS and of great benefit to the energy delivering of the high-power laser pulses. To the best of our knowledge, this is the first time to experimentally demonstrate the self-pumped SBS of high-power super-Gaussian-shaped laser pulses.

Keywords: Self-pumped SBS; High-power lasers; Super-Gaussian-shaped laser pulses

1. INTRODUCTION

Inertial confinement fusion (ICF) attracts the attention of researchers from all over the world because it can generate huge energy and should become an important way to solve the upcoming energy crisis. Fuel gain exceeding unity in an inertial confined fusion experiment was reported last year (Hurricane *et al*., 2014), marking that the research of ICF has stepped into a new stage. In the research of ICF, to get good homogeneity of irradiation in the ignition process, flat-topped (super-Gaussian-shaped) pulses are demanded for compressing the target (Wilcox *et al*., 1993; Radha *et al*., 2011; Hohenberger *et al*., 2014).

High-power laser pulses could excite different kinds of nonlinear effects when propagating in a nonlinear medium, and stimulated Brillouin scattering (SBS) is most likely to be excited for its relative lower threshold (Bai *et al*., 2008; Gao *et al*., 2010; Omatsu *et al*., 2012). The excitation of SBS may lead to the loss of energy and the damage of optical elements. According to the Fourier transform, there is a sideband in the spectrum of pulse with sharp edges. When the pump is reflected by optical elements in the light path, Stokes component in the reflected light would act as a weak seed injected in the opposite direction of the pump (Guo *et al*., 2005; Zhu *et al*., 2012; 2014). The existence of the weak seed would speed up the initiation progress of SBS, causing an adverse impact on the propagation of laser pulses.

In recent years, some research groups have reported that feedback in the opposite direction of the pump could lower the threshold of SBS and speed up the SBS excitation process. It is reported theoretically and experimentally that the SBS threshold could be reduced by half with the feedback of reflecting mirror at the output end of the Brillouin medium (Ajiya *et al*., 2009; Al-Asadi *et al*., 2010). They believed the reason is that the interaction length between the pump and Stokes light increases with the existence of pump recycling, so a relatively lower pump power is enough to excite SBS. Dement'ev *et al*. studied the influence of feedback caused by reflecting mirror at the back end of the medium cell on pulse compression (Dement'ev *et al*., 2011). They experimentally compressed 1 ns laser pulses to below 60 ps with counterpropagating pulses of the same carrier frequency and duration. Compared with the traditional SBS pulse compression, narrower pulse, lower SBS threshold, better energy stability, and time stability can be obtained

Address correspondence and reprint requests to: Zhiwei Lu, National Key Laboratory of Science and Technology on Tunable Laser, Harbin Institute of Technology, P. O. Box 3031, Harbin 150080, China. E-mail: zw_lu@sohu.com

[†]Yulei Wang and Xuehua Zhu contributed equally to this work.

with this technology. Kong *et al*. claimed that in the Brillouin medium the interaction between the forward-propagating pump and the backward-propagating feedback light can drive acoustic wave phase grating (Kong *et al*., 2005, 2007, 2009; Omatsu *et al*., 2012). The grating would scatter the pump and result in phase locking of Stokes light, which is called self-phase-locking SBS. This method could experimentally keep phase error of the scattered light below $\lambda/4$. Nevertheless, none of researches has ever mentioned the relationship between spectral characteristics of the pump and self-pumped SBS.

In this paper, beginning with spectral characteristics of the super-Gaussian-shaped laser pulses, we studied theoretically and experimentally on the self-pumped SBS. Our goal is to find out an optimum condition for effective delivering of this kind of laser pulses in a nonlinear optical medium. The 3 ns super-Gaussian-shaped pulses were chosen to work as the pump and FC-40 as the nonlinear medium. Firstly, the Fourier transform was used to study the spectrum of different-order super-Gaussian-shaped pulses, and intensity of Stokes component is quantified. Then a theoretical model was established to describe the self-pumped SBS. By numerically solving the model we obtained the self-pumped SBS intensity excited by different-order super-Gaussian-shaped pulses. Simulation results show that when super-Gaussian-shaped pulses whose order is lower than six propagate in a 600 mm medium cell, the self-pumped SBS effect can be suppressed. At last, we utilize a high-power Nd:glass laser system to conduct the relevant experiment, and the experimental results agree with calculated results of 20th-order super-Gaussian-shaped laser pulses.

2. NUMERICAL MODEL AND DISCUSSION

The waveforms and the related spectrum of 3 ns super-Gaussian-shaped laser pulses are shown in the insert of Figure 1. According to the Fourier transform, there exist sidelobes in the spectrum of super-Gaussian-shaped pulses. When these kind of pulses work as the pump of SBS, there is frequency component that fulfills Brillouin frequency shift of nonlinear medium in its sideband. Rayleigh scattering in the medium and reflection of rear cell window could result in the occurrence of back-propagating beam, and Stokes component in the back-propagating beam provides seed for exciting the SBS, this process is called self-Stokes seeding (Guo *et al*., 2005).

To numerically simulate the SBS initiated by Stokes component in the spectrum of the pump when propagating in the medium, we study the following coupled-wave equations describing this process (Boyd *et al*., 1990):

$$\frac{\partial A_1}{\partial z}+\frac{n}{c}\frac{\partial A_1}{\partial t}=i\frac{\omega\gamma_e}{4nc\rho_0}\rho A_2 \tag{1}$$

$$-\frac{\partial A_2}{\partial z}+\frac{n}{c}\frac{\partial A_2}{\partial t}=i\frac{\omega\gamma_e}{4nc\rho_0}\rho^* A_1 \tag{2}$$

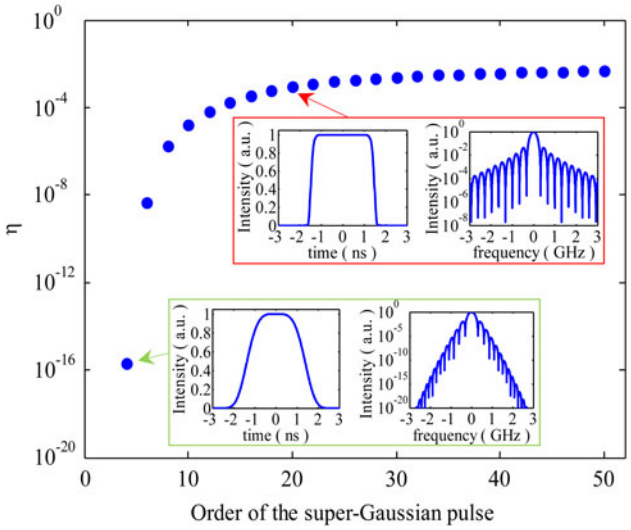

Fig. 1. Stokes component's proportion of total pulse energy of different-order super-Gaussian-shaped pulses. Insert: waveform and spectrum of 4th- and 20th-order super-Gaussian-shaped pulses.

$$\frac{\partial\rho}{\partial t}+\Gamma\rho=\frac{\gamma_e q^2}{16\pi\Omega_B}A_1A_2^*+f \tag{3}$$

Here A_1, A_2, and ρ respectively donate the amplitude of the pump, Stokes light and acoustic wave; n is the refractive index of Brillouin medium; c is the velocity of light in vacuum; ω is the angular frequency of the pump; ρ_0 is the medium density without laser injecting; γ_e is the electrostrictive constant; $\mathbf{q}$ is the wave vector of acoustic wave; Ω_B and Γ respectively donate the Brillouin frequency shift and Brillouin linewidth. With these parameters the gain factor can be calculated by $g_B=\gamma_e^2\omega^2/nc^3V\rho_0\Gamma$, and V donates the velocity of sound in the medium. f represents the Langevin noise source that describes the random thermal noise in the medium$\langle f(z,\ t)\rangle=0$, and it follows the relation and $\langle f(z,\ t)f^*(z',\ t')\rangle=Q\delta(z-z')\delta(t-t')$, in which $Q=2kT\rho_0\Gamma/V^2A$, k is the Boltzmann constant, T is the temperature of the medium and A is the cross-sectional area of the beam (Boyd *et al*., 1990).

By numerically the solving coupled-wave equations consisting of (1)–(3), we can model the SBS process when the pump is injected into the medium cell. Initial conditions of needed parameters are given below. In the discrete case, noise source f in Eq. (3) can be presented as (Zeringue *et al*., 2012): $\boldsymbol{f}_{j,k}=\sqrt{nQ/(\Delta t)^2c}\mathbf{S}_{j,k}$, where j and k respectively represent the temporal and spatial grid points, $\mathbf{S}_{j,k}$ is the Gaussian random matrix whose average is 0 and variance is 1, Δt is the time-step. Initial conditions of the pump are $A_1(j=0,k)=A_0$ and $A_1(j>0,k=0)=0$; here $j=0$ corresponds to $z=0$, $k=0$ corresponds to $t=0$, and A_0 is the waveform of incident the pump. Reflection of rear cell window should be introduced and we assume that the reflectivity is r, besides, the proportion of Stokes component among the pump is taken as η, the initial conditions of

https://doi.org/10.1017/S0263034615000920 Published online by Cambridge University Press

Stokes light can be described as:

$$A_2(j = N_j, k) = \begin{cases} r\eta A_1(j = 0, k - [T_t/\Delta t]), & k > [T_t/\Delta t] \\ 0, & \text{others} \end{cases}$$

$$A_2(j < N_j, k) = 0$$

in which T_t represents the propagation time of the laser pulse in a medium, N_j corresponds to $z = L$ and [ ] represents to round numbers. At last, initial conditions of acoustic wave are given as:

$$\rho(j = 0, k) = f_{0,k}$$

$$\rho(j, k = 0) = f_{j,0}$$

The parameters used in our numerical calculation are shown in Table 1, and the Brillouin medium is heavy fluorocarbon FC-40. In the parameters, the refractive index and gain coefficient are presented in formal articles (Yoshida *et al*., 2009; Zhu *et al*., 2015). Moreover, the phonon lifetime and Brillouin shift are calculated from the corresponding parameters in (Yoshida *et al*., 2009).

For different order of super-Gaussian-shaped laser pulses, the ratios (η) between energy of Stokes component and total pulse energy are shown in Figure 1. When the order is lower than 20, η increases significantly with the increase of the order; after the order exceeds 20, η tends to become a constant. For 20th-order super-Gaussian-shaped laser pulses, η is approximately 8.9×10^{-4}. In the medium cell, reflectivity of the rear window could be calculated to be approximately 10^{-3} according to the Fresnel formula; thus, the intensity of the Stokes component is 8.9×10^{-7} times that of the pump.

3. SIMULATION RESULTS

3.1 Self-pumped SBS of 3 ns, 20th-order super-Gaussian-shaped pulses

According to the theoretical model and the parameters mentioned above, numerical simulation of the reflected light was carried out with different pump intensities (see Fig. 2). When the pump intensity is relatively low (below 780 MW/cm^2), there is only one reflected peak near 8 ns in the waveform of reflected light, and the intensity of this peak increases with the rise of pump intensity. When pump intensity is higher than 780 MW/cm^2, another reflected peak occurs about 2 ns ahead of the pre-existing pulse, and the waveform of the reflected light presents a double-peak structure. According to the model proposed above, in this double-peak structure the first pulse (pulse between 5 and 6 ns) is the component initiated by randomly distributed thermal noise when a 3 ns super-Gaussian-shaped pulse propagates in the medium, the second pulse (pulse near 8 ns) is the above-mentioned self-pumped SBS. Waveform of the reflected light when pump intensity equals 1150 MW/cm^2 is shown as the insert of Figure 2. There exist two reflected peaks in the waveform, and the delay between the two peaks is 2.35 ns.

Given that the pump pulses are super-Gaussian-shaped with 3 ns duration, in a non-focusing-pumped scheme the distance between start position of noise-initiated SBS light and the front cell window is equal to the spatial length corresponding to half of pump pulse-duration. This distance could be calculated to be approximately 35 cm with the refractive index of FC-40. Keep in mind that the length of the medium cell is 60 cm. The pump that has not been depleted by noise-initiated SBS continues to propagate and is reflected by the rear cell window. Then the Stokes component in the reflected light works as a seed to form the second pulse. The delay between the two pulses equals the time needed for the laser to pass twice the medium between the start position of noise-initiated SBS and the rear cell window. As shown in Figure 3, time between two pulses increases exponentially with the rising of pump intensity. When pump intensity is near the noise-initiated SBS threshold, the delay equals to the time needed for laser passing twice 25 cm-long medium in the latter half of the medium cell back and forth, approximately 2.13 ns. With the increase of pump intensity, the generation of noise-initiated SBS calls for a more smaller medium length, such that the distance between the start position and rear cell window increases, and the delay between two pulses gradually increases, as seen in Figure 3.

Energy reflectivity with different pump intensity is calculated and shown in Figure 4. The chain line is the energy reflectivity curve of the first reflected peak (noise-initiated SBS), the dotted line represents energy reflectivity of the second reflected peak (self-pumped SBS), and the solid line is the total energy reflectivity curve (noise-initiated SBS + self-pumped SBS). It suggests that when pump intensity is below 780 MW/cm^2, there is no noise-initiated SBS exists, and the self-pumped SBS contributes to the total energy reflectivity. The energy reflectivity monotonically increases with the increase of pump intensity. When pump intensity is higher than 780 MW/cm^2, the noise-initiated SBS starts to occur and its reflectivity increases nonlinearly with

Table 1. *Simulation parameters*

Description	Parameter
Laser wavelength, λ	527 nm
Pulse-width, t_p	5 ns
Beam diameter, D	20 mm
Refractive index, n	1.28
Cell length, L	60 cm
Brillouin gain coefficient, g	2 cm/GW
Brillouin shift, Ω_B	2162 MHz
Brillouin bandwidth, Γ_B	410 MHz
Phonon lifetime, τ_B	60 ps

https://doi.org/10.1017/S0263034615000920 Published online by Cambridge University Press

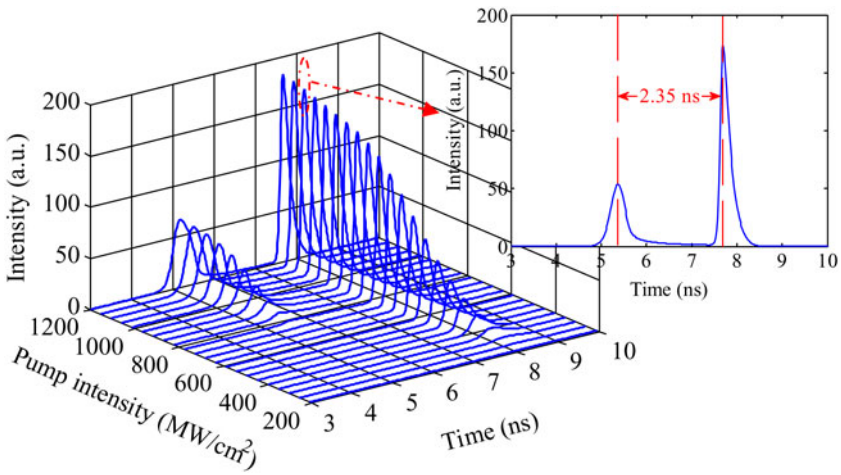

Fig. 2. Simulated waveforms of the reflected pulses with different pump intensity.

the rise of pump intensity; energy reflectivity of the self-pumped SBS increases more slowly, and then starts to decrease while the total energy reflectivity continues to rise. The reason is that after noise-initiated SBS occurs, its intensity increases nonlinearly with the rise of pump intensity and extracts most pump energy, resulting in the decrease of pump energy used to generate the self-pumped SBS. When the pump intensity exceeds 1200 MW/cm^2, energy reflectivity of noise-initiated SBS exceeds that of the self-pumped SBS. It can be predicted that if pump intensity is high enough, nearly all of pump energy should be used to form the first reflected peak, and the second one will disappear.

3.2 Influence of the order of super-Gaussian-shaped pulses on self-pumped SBS

Figure 5a shows the relationship between self-pumped SBS reflectivity and pump intensity when different-order super-Gaussian-shaped pulses propagate in the medium cell. When pump intensity is fixed, with the increase of the order, reflectivity of self-pumped SBS gradually increases, and self-pumped SBS threshold (generally defined as incident laser intensity corresponding to 1% reflectivity) gradually decreases. As discussed above, the reason for this phenomenon is that higher-order super-Gaussian-shaped pulses contain stronger Stokes component, and provide a more stronger seed for SBS. The maximum reflectivity of different-order super-Gaussian-shaped pulses is shown in Figure 5b. Lower order will lead to lower maximum reflectivity of self-pumped SBS, and benefits the propagation of laser pulses in the nonlinear medium. When the order is lower than 6, the maximum reflectivity of self-pumped SBS is controlled below 2%, which means that the influence of this nonlinear effect on laser propagation is negligible, and the noise-initiated SBS takes hold.

When pump intensity is 660 MW/cm^2, for two different kinds of super-Gaussian-shaped pulses, waveform of incident pulse and transmitted pulse are illustrated in Figure 6

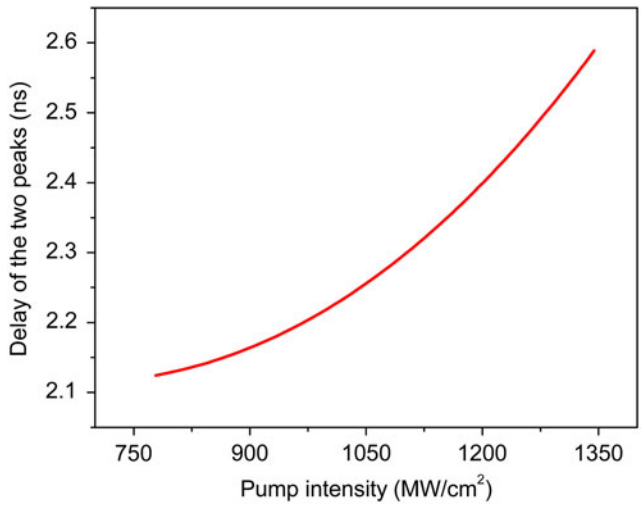

Fig. 3. Delay between two peaks of reflected light waveform.

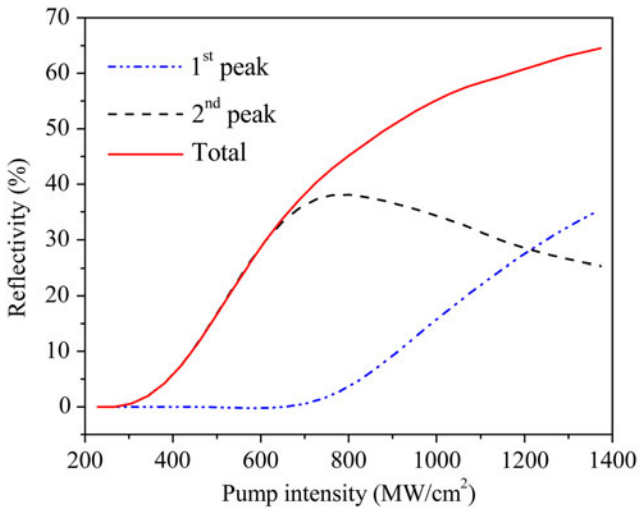

Fig. 4. Energy reflectivity with different pump intensity.

https://doi.org/10.1017/S0263034615000920 Published online by Cambridge University Press

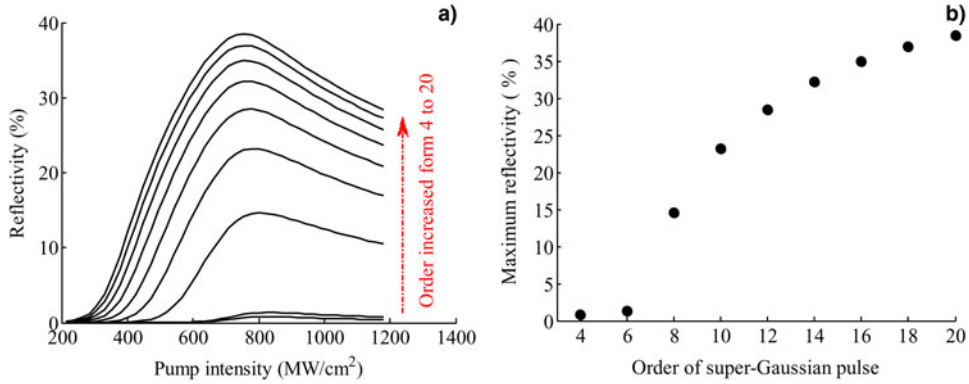

Fig. 5. Reflectivity curves of different order super-Gaussian-shaped pulses (**a**) and maximum reflectivity obtained (**b**).

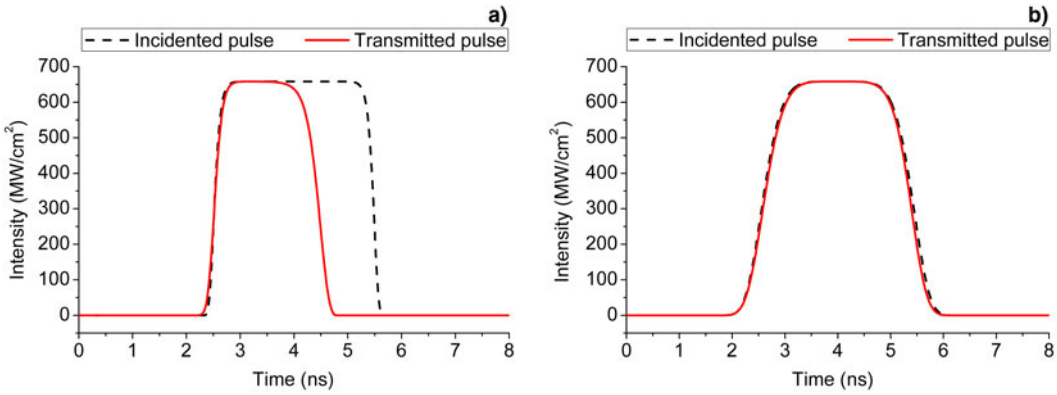

Fig. 6. Waveform of incident pulse and transmitted pulse: (**a**) 20th-order super-Gaussian-shaped pulse, (**b**) 6th-order super-Gaussian-shaped pulse.

with solid and dotted lines, respectively. It is shown that for the 20th-order super-Gaussian-shaped pulses, a great extent loss of energy takes place at pulse trailing owing to self-pumped SBS, laser pulse distorts obviously. However, waveform of the 6th-order super-Gaussian-shaped pulses remains nearly unchanged in the propagation process. The waveform fidelity is well, and the corresponding reflectivity is close to zero. These also indicate that the 6th-order super-Gaussian-shaped pulses benefit energy delivering from their time characteristics.

4. EXPERIMENTAL RESULTS AND DISCUSSION

We carried out an experiment on self-pumped SBS with frequency-selective amplification of super-Gaussian-shaped laser pulses, and the experimental setup is shown in Figure 7. A high-power Nd:glass laser system is used as pump source in the experiment, the output pulse is flat-top-shaped with a duration of 3 ns, the beam diameter is approximately 60 mm, the wavelength is 527 nm, and the single-pulse energy is over 10 J. A 3:1 beam-contracting system is used to enhance the intensity of laser. By doing this, the beam diameter is reduced to 20 mm and the laser intensity is magnified nine times. Laser near-field pattern after beam contracting is shown as the insert. Laser pulse outputs from the beam-contracting system and is sampled by a wedge plate, and then it is introduced into the medium cell and induces SBS. A part of the laser is sampled by the first surface of the wedge plate and irradiates onto the energy detector ED1 (PE50DIF-ER, Ophir). The energy is recorded as E_0, if the sampling rate of the wedge plate is measured to be k, pump energy that enters medium cell is $E_p = (1 - k) \cdot E_0$. Reflected light of the second surface of the wedge plate is detected by a photoelectric (Alphalas, UPD-40-UVIR-D, risetime <40 ps) and is recorded by a digital oscilloscope (Tektronix DPO71254, bandwidth 12.5 GHz, sample rate 100 Gs/s). Length of the medium cell is 600 mm, both quartz windows of the cell are anti-reflection coated on the outer side, and the cell is filled with FC-40. The pump passes through the front cell window and propagates in the medium, and then is reflected by the interface between the medium and rear cell window. Stokes component in the reflected light is amplified by the subsequent pump and is output from the front window. Then the reflected light is sampled by the wedge plate again, and its energy and waveform are recorded by ED2 and PD2, respectively. The energy

https://doi.org/10.1017/S0263034615000920 Published online by Cambridge University Press

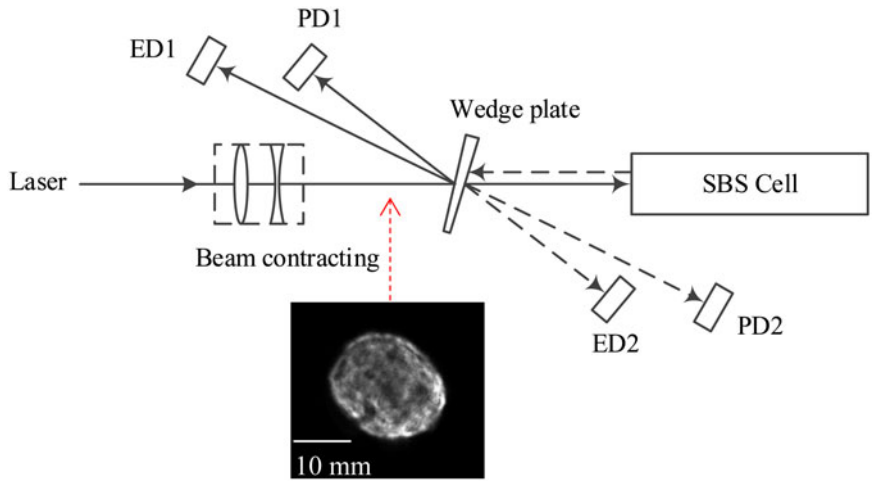

Fig. 7. Schematic diagram of the experimental setup. Beam contracting system: 3:1 (1500 & −500 mm); ED1, ED2: energy detectors; PD1, PD2: photoelectric detectors.

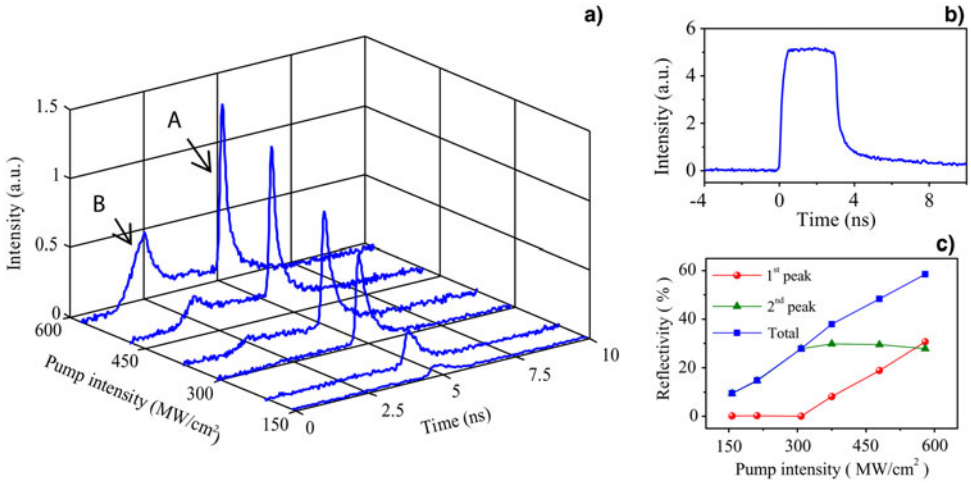

Fig. 8. Typical waveforms measured in the experiment: (**a**) waveforms of reflected light, (**b**) waveforms of the pump, (**c**) energy reflectivity of each peak in waveform of reflected light and total energy reflectivity.

detector and photoelectric detector are the same as those used for measuring the pump parameters.

Typical waveforms measured in the experiment with different pump intensities are shown in Figure 8, as well as the energy reflectivity of each peak in reflected waveform and the total energy reflectivity. Figure 8b illustrates the typical pump waveform, which is nearly super-Gaussian-shaped with pulse duration of 3 ns. Figure 8a illustrates typical waveforms of the reflected light. When pump intensity is relatively low, the reflected waveform takes a single-peak structure, marked as pulse A. When pump intensity reaches 375 MW/cm^2, another pulse component appears in front of pulse A, which is marked as pulse B. With the increase of pump intensity, the intensities of both of the two pulses increase gradually. It is also shown in Figure 8 that the delay between two pulses is approximately 2.5 ns, which is close to the calculated results. There is still a derivation because some error exists in the measurement of pulse duration and medium parameters.

Energy reflectivity of pulse A, B, and total energy reflectivity are shown in Figure 8c. When pump intensity is below 308 MW/cm^2, only pulse A contributes to the total energy reflectivity, which grows monotonously with the increase of pump energy. Then with the continuously increasing of pump intensity, pulse B appears and the energy reflectivity grows nonlinearly. At the same time energy reflectivity of pulse A increases more slowly and then tends to decrease, which agrees with the above simulation results.

For large-aperture laser beams, the uniformity of transverse intensity distribution directly affects the SBS process. Backscattering initiates mainly in the spots with high intensity (hot-spots) in the beam aperture. Thus, estimating SBS process with the average intensity will get a low accuracy. Skeldon and Bahr proposed that the practical intensity

https://doi.org/10.1017/S0263034615000920 Published online by Cambridge University Press

should be equal to average intensity multiplied by a hot-spot parameter (Skeldon & Bahr, 1991). According to the near-field pattern in the insert of Figure 7, the hot-spot parameter is approximately 1.8. If we multiply the pump intensity in Figure 8 by 1.8, a reasonable agreement between the experimental results and the numerical calculations, shown in Figures 3 and 4, would be obtained.

5. CONCLUSIONS

Theoretical and experimental study of self-pumped SBS caused by a 3 ns super-Gaussian-shaped laser pulse is demonstrated in this paper. With heavy fluorocarbon liquid FC-40 as a nonlinear medium and for 3 ns different-order super-Gaussian-shaped pulses, we calculated the Stokes component proportion of total laser pulse energy with the Fourier transform. We established a theoretical model to describe the self-pumped SBS and numerically calculated the evolution process of SBS when a super-Gaussian-shaped pulse is injected into the medium cell. The results show self-pumped SBS of lower-order super-Gaussian-shaped laser pulses is relatively weak, which benefits the propagation of high-power laser pulses. A sixth-order super-Gaussian-shaped pulse can traverse the 60 cm medium cell without exciting the self-pumped SBS. In the experiment, high-power Nd:glass laser system with 527 nm wavelength works as light source, and output 3 ns super-Gaussian-shaped laser pulses with over 10 J single-pulse energy. A 600 mm long medium cell was filled with FC-40. Self-pumped SBS was observed in the experiment, and the evolution process agreed well with the calculated results. The results of this paper have guiding significance for the design of high-power laser systems to avoid energy loss and elements damage caused by such nonlinear optical effects.

ACKNOWLEDGMENTS

This work is supported by the National Natural Science Foundation of China (Grant No. 61138005 and No. 61378007).

REFERENCES

Ajiya, M., Mahdi, M.A., Al-Mansoori, M.H., Shee, Y.G., Hitam, S. & Mokhtar, M. (2009). Reduction of stimulated Brillouin scattering threshold through pump recycling technique. *Laser Phys. Lett.* **6**, 535–538.

Al-Asadi, H., Al-Mansoori, M., Ajiya, M., Hitam, S., Saripan, M. & Mahdi, M. (2010). Effects of pump recycling technique on stimulated Brillouin scattering threshold: A theoretical model. *Opt. Express* **18**, 22339–22347.

Bai, J.H., Shi, J.W., Ouyang, M., Chen, X.D., Gong, W.P., Jing, H.M., Liu, J. & Liu, D.H. (2008). Method for measuring the threshold value of stimulated Brillouin scattering in water. *Opt. Lett.* **33**, 1539–1541.

Boyd, R.W., Rzazewski, K. & Narum, P. (1990). Noise initiation of stimulated Brillouin scattering. *Phys. Rev. A* **42**, 5514–5521.

Dement'ev, A.S., Demin, I., Murauskas, E. & Slavinskis, S. (2011). Compression of pulses during their amplification in the field of a focused counterpropagating pump pulse of the same frequency and width in media with electrostriction nonlinearity. *Quantum Electron.* **41**, 153.

Gao, W., Lu, Z.W., Wang, S.Y., He, W.M. & Hasi, W.L.J. (2010). Measurement of stimulated Brillouin scattering threshold by the optical limiting of pump output energy. *Laser Part. Beams* **28**, 179–184.

Guo, S.F., Lu, Q.S., Cheng, X.A., Zhou, P., Deng, S.Y. & Yin, Y. (2005). Influence of Stokes component in reflected light on stimulated Brillouin scattering process. *Acta Phys. Sin.* **53**, 1831–1835.

Hohenberger, M., Theobald, W., Hu, S.X., Anderson, K.S. & Betti, R. (2014). Shock-ignition relevant experiments with planar targets on OMEGA. *Phys. Plasmas* **21**, 022702.

Hurricane, O.A., Callahan, D.A., Casey, D.T., Celliers, P.M., Cerjan, C., Dewald, E.L., Dittrich, T.R., Doppner, T., Hinkel, D.E., Hopkins, L.F.B., Kline, J.L., Le Pape, S., Ma, T., MacPhee, A.G., Milovich, J.L., Pak, A., Park, H.S., Patel, P.K., Remington, B.A., Salmonson, J.D., Springer, P.T. & Tommasini, R. (2014). Fuel gain exceeding unity in an inertially confined fusion implosion. *Nature* **506**, 343–348.

Kong, H.J., Lee, S.K., Lee, D.W. & Guo, H. (2005). Phase control of a stimulated Brillouin scattering phase conjugate mirror by a self-generated density modulation. *Appl. Phys. Lett.* **86**, 051111.

Kong, H.J., Shin, J.S., Yoon, J.W. & Beak, D.H. (2009). Phase stabilization of the amplitude dividing four-beam combined laser system using stimulated Brillouin scattering phase conjugate mirrors. *Laser Part. Beams* **27**, 179–184.

Kong, H.J., Yoon, J.W., Beak, D.H., Shin, J.S., Lee, S.K. & Lee, D.W. (2007). Laser fusion driver using stimulated Brillouin scattering phase conjugate mirrors by a self-density modulation. *Laser Part. Beams* **25**, 225–238.

Omatsu, T., Kong, H.J., Park, S., Cha, S., Yoshida, H., Tsubakimoto, K., Fujita, H., Miyanaga, N., Nakatsuka, M., Wang, Y., Lu, Z., Zheng, Z., Zhang, Y., Kalal, M., Slezak, O., Ashihara, M., Yoshino, T., Hayashi, K., Tokizane, Y., Okida, M., Miyamoto, K., Toyoda, K., Grabar, A.A., Kabir, M.M., Oishi, Y., Suzuki, H., Kannari, F., Schaefer, C., Pandiri, K.R., Katsuragawa, M., Wang, Y.L., Lu, Z.W., Wang, S.Y., Zheng, Z.X., He, W.M., Lin, D.Y., Hasi, W.L.J., Guo, X.Y., Lu, H.H., Fu, M.L., Gong, S., Geng, X.Z., Sharma, R.P., Sharma, P., Rajput, S., Bhardwaj, A.K., Zhu, C.Y. & Gao, W. (2012). The Current Trends in SBS and phase conjugation. *Laser Part. Beams* **30**, 117–174.

Radha, P.B., Betti, R., Boehly, T.R., Delettrez, J.A., Edgell, D.H., Goncharov, V.N., Igumenshchev, I.V., Knauer, J.P., Marozas, J.A., Marshall, F.J., McCrory, R.L., Meyerhofer, D.D., Regan, S.P., Sangster, T.C., Seka, W., Skupsky, S., Solodov, A.A., Stoeckl, C., Theobald, W., Frenje, J.A., Casey, D.T., Li, C.K. & Petrasso, R.D. (2011). Inertial confinement fusion using the omega laser system. *IEEE Trans. Plasma Sci.* **39**, 1007–1014.

Skeldon, M.D. & Bahr, R. (1991). Stimulated rotational raman-scattering in air with a high-power broad-band laser. *Opt. Lett.* **16**, 366–368.

Wilcox, R.B., Behrendt, W., Browning, D.F., Speck, D.R. & Van-Wonterghem, B.M. (1993). Fusion laser oscillator and pulse-forming system using integrated optics. *Proc. SPIE* **1870**, 53–63.

Yoshida, H., Hatae, T., Fujita, H., Nakatsuka, M. & Kitamura, S. (2009). A high-energy 160-ps pulse generation by stimulated Brillouin scattering from heavy fluorocarbon liquid at 1064 nm wavelength. *Opt. Express* **17**, 13654–13662.

Zeringue, C., Dajani, I., Naderi, S., Moore, G.T. & Robin, C. (2012). A theoretical study of transient stimulated Brillouin scattering in optical fibers seeded with phase-modulated light. *Opt. Express* **20**, 21196–21213.

Zhu, X., Lu, Z. & Wang, Y. (2015). High stability, single frequency, 300 mJ, 130 ps laser pulse generation based on stimulated Brillouin scattering pulse compression. *Laser Part. Beams* **33**, 11–15.

Zhu, X., Wang, Y. & Lu, Z. (2014). Measurement of the threshold of nonfocusing-pumped stimulated Brillouin scattering based on temporal characteristic of the reflected pulse. *Appl. Phys. Express* **7**, 122601.

Zhu, X.H., Lu, Z.W. & Wang, Y.L. (2012). A new method for measuring the threshold of stimulated Brillouin scattering. *Chin. Phys. B* **21**, 074205.

https://doi.org/10.1017/S0263034615000920 Published online by Cambridge University Press